nature neuroscience

Anisotropic encoding of three-dimensional space by place cells and grid cells

Robin Hayman[1,5], Madeleine A Verriotis[1,5], Aleksandar Jovalekic[1,4,5], André A Fenton[2,3] & Kathryn J Jeffery[1]

The subjective sense of space may result in part from the combined activity of place cells in the hippocampus and grid cells in posterior cortical regions such as the entorhinal cortex and pre- and parasubiculum. In horizontal planar environments, place cells provide focal positional information, whereas grid cells supply odometric (distance measuring) information. How these cells operate in three dimensions is unknown, even though the real world is three-dimensional. We investigated this issue in rats exploring two different kinds of apparatus: a climbing wall (the 'pegboard') and a helix. Place and grid cell firing fields had normal horizontal characteristics but were elongated vertically, with grid fields forming stripes. It seems that grid cell odometry (and by implication path integration) is impaired or absent in the vertical domain, at least when the rat itself remains horizontal. These findings suggest that the mammalian encoding of three-dimensional space is anisotropic.

© 2011 Nature America, Inc. All rights reserved.

Neural encoding of position is a core cognitive competence that depends on activity in a network of structures centered on the hippocampal formation[1]. Hippocampal place cells encode position, with localized activity occurring in one or (sometimes) a few locations[2]. Upstream of these cells, neurons in posterior cortical areas, such as the entorhinal cortex[3] and pre- and parasubiculum[4], produce extensive, evenly spaced firing arrays, called grids, that provide place cells with metric (distance and direction) information. These 'grid cells' derive their information, in turn, from a mixture of self-motion cues (path integration) and learned landmarks[3,5]. Because of their metric properties, grid cells provide an opportunity to elucidate the fundamental metric structure of the mammalian spatial representation (the cognitive map[6]).

The properties of the cognitive map on the horizontal plane have been extensively studied, but animals move in three dimensions, and three-dimensional movement poses computational challenges that are not present in two dimensions[7]. For example, movement on a slope results in a smaller horizontal translation per unit surface distance covered, and the outcome of rotations in three dimensions depends on the order in which they are executed (that is, the operation is non-commutative). This raises the question of how the mapping system tracks position for animals moving in non-horizontal environments. Grid cells, because of their odometric properties, offer a window into this issue. We show here that place and grid cells exhibit a relative insensitivity to height, with grid cells being even less sensitive than place cells. The cognitive map is thus anisotropic, encoding vertical space differently from horizontal. We suggest that the mammalian cognitive map may be a contextually modulated two-dimensional map (or set of maps) rather than a true volumetric representation.

RESULTS

We used parametric statistical tests throughout but verified these with more conservative non-parametric tests in cases of skewed distribution; we found no differences between these tests, and so the analyses to follow report the parametric test results. Numbers report mean ± s.e.m. unless otherwise stated, and the results are summarized in **Table 1**.

In experiment 1 (**Fig. 1**), we recorded place cells from the hippocampal CA1 region and grid cells from posterior cortex as rats foraged over the pegboard, a vertically oriented arena with projecting pegs (**Fig. 1e** and **Supplementary Fig. 1a**). We made comparisons with recordings from horizontal environments.

Place fields on the vertical arena

We recorded 40 place cells from seven rats on the pegboard and compared their firing rates with 53 cells from five rats recorded on flat arenas. Thirty-one cells from four rats were recorded in both settings. Place cells fired readily on the pegboard, producing delimited elliptical areas of activity ('place fields'), indicating sensitivity to height as well as horizontal position (**Fig. 1a**; see **Supplementary Fig. 2** for the complete data set). Both major and minor axes (length and width, respectively) of the fields were significantly larger on the pegboard (major axes = 78 ± 3 cm on the pegboard and 38 ± 2 cm on the flat arenas; Student's *t*-test: $t_{91} = 11.0$, $P < 0.0001$; minor axes = 39 ± 3 cm on the pegboard and 21 ± 1 cm on the flat; $t_{91} = 6.1$, $P < 0.0001$). Place fields on the flat arenas were, as is typical of place fields, slightly oval, with an aspect ratio of 2.0 ± 0.1, consistent with previous measurements[8]. On the pegboard the place fields were more elongated, with an aspect ratio of 2.4 ± 0.2, significantly greater than that on the flat arenas ($t_{91} = 2.2$, $P < 0.05$; **Fig. 1b**). Because place fields on the pegboard were mostly aligned vertically, in contrast with the horizontal arenas (**Fig. 1c**), it follows that this elongation occurred in the vertical dimension. This was verified by determining the vertical:horizontal span of the fields and comparing this with the ratio obtained by choosing 'vertical' and 'horizontal' directions on

[1]Institute of Behavioural Neuroscience, Department of Cognitive, Perceptual and Brain Sciences, Division of Psychology and Language Sciences, University College London, London, UK. [2]Center for Neural Science, New York University, New York, New York, USA. [3]Department of Physiology and Pharmacology, State University of New York, Brooklyn, New York, USA. [4]Axona Ltd, Herts, UK. [5]These authors contributed equally to this work. Correspondence should be addressed to K.J.J. (k.jeffery@ucl.ac.uk).

Received 11 January; accepted 7 July; published online 7 August 2011; doi:10.1038/nn.2892

Table 1 Comparison of firing field characteristics for place and grid cells on apparatuses of differing form and dimensionality

		Place fields			Grid fields		
		n	Mean	S.e.m.	*n*	Mean	S.e.m.
Peak firing rate (Hz)	Flat arenas	53	9.8	0.9	23	7.8	1.4
	Pegboard	40	5.1	0.5	17	5.6	1.3
	Helix	103	10.3	0.7	53	9.5	1.0
Major axis or height (cm)	Flat arenas	53	38	2	23	52	5
	Pegboard	40	78	3	17	98	4
	Helix (five-coil)	50	63	2	53	69	1
	Helix (six-coil)	53	75	2	–	–	–
	Helix (all)	103	69	2	53	69	1
Minor axis or width (cm)	Flat arenas	53	21	1	23	35	4
	Pegboard	40	39	3	17	38	3
	Helix (five-coil)	50	35	3	53	28	2
	Helix (six-coil)	53	45	4	–	–	–
	Helix (all)	103	40	2	53	28	2
Aspect ratio	Flat arenas	53	2.0	0.1	23	1.5	0.1
	Pegboard	40	2.4	0.2	17	3.0	0.4
	Helix (five-coil)	50	2.2	0.1	53	2.9	0.1
	Helix (six-coil)	53	2.1	0.1	–	–	–
	Helix (all)	103	2.1	0.1	53	2.9	0.1
Skaggs information[a] (total bits per spike)	Flat arenas	53	1.63	0.10	23	1.00	0.09
	Pegboard	40	1.16	0.10	17	0.77	0.07
Skaggs information (horizontal bits per spike)	Flat arenas	53	0.64	0.06	23	0.29	0.04
	Pegboard	40	0.66	0.06	17	0.55	0.06
Skaggs information (vertical bits per spike)	Flat arenas	53	0.56	0.04	23	0.25	0.03
	Pegboard	40	0.24	0.02	17	0.17	0.03

[a]Obtained using Skaggs' method[9].

the flat arenas arbitrarily: the difference remained (pegboard ratio = 1.8 ± 0.1, flat ratio = 1.4 ± 0.1; $t_{91} = 2.6$, $P < 0.01$).

Spatial information was compared between vertical and horizontal dimensions using Skaggs' method[9] (see Online Methods for details) by collapsing the firing rate maps to a linear array either vertically or horizontally (**Fig. 1d**). On the flat arenas the scores for the two dimensions were 0.64 ± 0.06 and 0.56 ± 0.04 bits for the arbitrary 'horizontal' and 'vertical', respectively, which did not differ ($t_{67} = 1.39$, not significant). For the pegboard, the horizontal and vertical information scores were 0.66 ± 0.06 and 0.24 ± 0.02 bits, respectively, which were highly significantly different ($t_{46} = 6.86$, $P < 0.001$). Thus, place field information content was higher in the horizontal direction than in the vertical direction for the vertical arena (the pegboard).

To assess place field modulation by height, the pegboard was binned into five horizontal layers (**Fig. 1e**) and firing rates (as a percentage of peak) were calculated for each cell on each layer: 19 out of 40 fields spanned all five layers and 21 out of 40 spanned fewer than five layers (**Fig. 1f**). The fields, despite their elongation, were partially height-modulated, as even when the peak layer was excluded, the intensity of individual fields fell steadily with increasing distance from the peak rather than simply fluctuating (**Supplementary Fig. 3**; $R = -0.55$, $P < 0.0001$).

Grid fields on the vertical arena

We recorded 17 grid cells from five rats on the pegboard and compared their firing characteristics with 34 cells from ten rats on flat arenas. Sixteen cells from five rats were recorded in both settings (**Fig. 2a**; see **Supplementary Fig. 4** for the complete data set). The cells produced grid-like periodic firing on the flat arenas (**Fig. 2a** and **Supplementary Fig. 4a–d**). They also fired on the vertical pegboard, but instead of producing vertical grids, they produced vertically aligned stripes (**Fig. 2** and **Supplementary Fig. 4e–h**). This elongation of the firing fields was reflected in their size and aspect ratio characteristics (**Table 1**): for the 23 cells having grids that could be analyzed quantitatively (**Supplementary Results**), major axes averaged 98 ± 4 cm on the pegboard, compared with 52 ± 5 cm on the flat arenas ($t_{38} = 6.7$, $P < 0.0001$). By contrast, minor axes did not differ, being 38 ± 3 cm on the pegboard and 35 ± 4 cm on the flat ($t_{38} = 0.5$, not significant), resulting in a significantly greater aspect ratio on the pegboard (3.0 ± 0.4) compared with the flat (1.5 ± 0.1; $t_{38} = 4.6$, $P < 0.0001$; **Fig. 2b**). As with the place cells, most of this difference could be accounted for by vertical stretching (**Fig. 2c**): the vertical:horizontal size ratio on the pegboard was 2.3 ± 0.2, whereas the (arbitrarily chosen) 'vertical':'horizontal' size ratio on the flat was significantly lower, at 1.2 ± 0.1 ($t_{38} = 4.7$, $P < 0.0001$). An analysis of variance (ANOVA) comparing the aspect ratios for 17 grid fields and 17 randomly selected place fields from the pegboard and flat conditions revealed no effect of cell type ($F_{1,64} = 0.5$, not significant) but a main effect of environment ($F_{1,64} = 11$, $P < 0.01$) and a significant cell × environment interaction ($F_{1,64} = 5.3$, $P < 0.05$). *Post hoc* pairwise analyses (Tukey's test) revealed that grid fields were significantly narrower than place fields on the flat ($t_{32} = 2.41$, $P < 0.05$) but not on the pegboard ($t_{32} = 1.58$, not significant). The vertical field size count showed that of the 17 grid fields, 13 spanned all five layers and only 4 spanned fewer than five layers (**Fig. 2e**). The elongation was significantly greater for grid cells than for place cells (chi-squared test of all five layers versus fewer than five layers for place and grid cells: $\chi^2_{1,N=57} = 4.07$, $P < 0.05$; **Fig. 2f**).

As with the place cells, grid field spatial information content was calculated for each dimension separately (**Fig. 2d**). On the flat arenas the (arbitrarily chosen) 'horizontal' and 'vertical' information scores were 0.29 ± 0.04 and 0.25 ± 0.03 bits, respectively, which did not differ ($t_{33} = 1.3$, not significant). For the pegboard, the horizontal and vertical information scores were 0.55 ± 0.06 and 0.17 ± 0.03 bits, respectively, which differed significantly ($t_{16} = 6.2$, $P < 0.0001$). Thus, the information content for grid cells was much lower in the vertical dimension on the vertical arena. Comparison of vertical information for grid cells and place cells on the pegboard found no difference ($t_{62} = 1.6$, not significant). A symmetry analysis (see Online Methods for details) found that grid cell firing fields had six-fold symmetry on the flat and two-fold symmetry on the pegboard (**Supplementary Fig. 5** and **Supplementary Results**).

The stripes resulted from the vertical orientation of the pegboard because, on the same apparatus laid horizontally, grid cells produced grids (**Supplementary Fig. 6**). To further rule out locomotor confounds, we classified the spike data from the pegboard trials according to whether the rat was moving up, down, left or right: stripes persisted in all travel directions (**Supplementary Fig. 7**).

We next looked to see whether the stripe spacing was similar to the spacing of the same cell's fields on a flat arena (**Supplementary Fig. 8**). For the 16 cells recorded on both arenas, we compared stripe width and spacing on the pegboard with that on the flat arenas. Stripe width averaged 37 ± 2 cm, and subfield width did not differ at 31 ± 7 cm ($t_{24} = 0.64$, not significant), and these values did not correlate

© 2011 Nature America, Inc. All rights reserved.

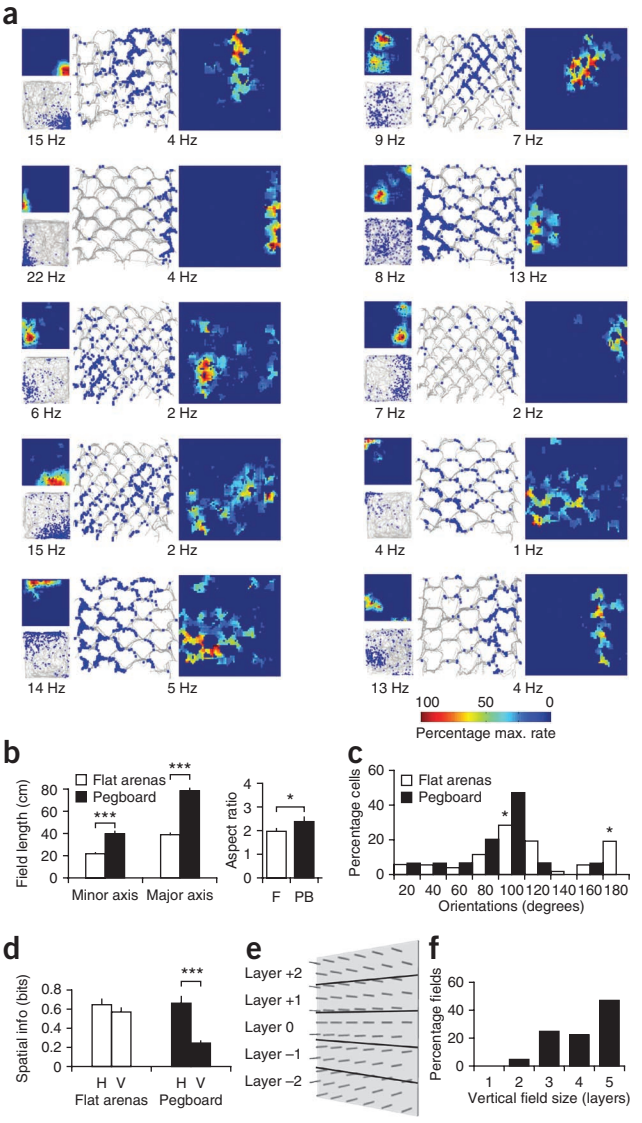

Figure 1 Place fields on the pegboard. (**a**) Firing fields of ten hippocampal place cells recorded in 60 cm square horizontal environments (leftmost pair in each group of plots) and on the 1.2 m square vertical pegboard (center and right in each group of plots). Each field is shown as raw data (black traces, rat's path; blue squares, superimposed action potentials) and as smoothed contour plots, with the corresponding peak rate (Hz) indicated below each pair of plots. The color bar shows percentages of peak firing. (**b**) Length (mean ± s.e.m.) of the major (long) and minor (short) axes, and aspect ratios (mean ± s.e.m.) of fields in the flat arenas and pegboard (F, flat; PB, pegboard) (*$P < 0.05$, ***$P < 0.0001$). (**c**) Orientations of place fields in the two environments. In the flat arenas, 90° was arbitrarily aligned with one pair of arena walls. Place field orientation showed two peaks (asterisks) at 90 and 180°, reflecting the tendency of place fields to align with walls. On the pegboard, almost all fields aligned vertically (90°). (**d**) One-dimensional spatial information content (mean ± s.e.m.) for firing rate maps collapsed horizontally (H) or vertically (V), in either flat arenas (H and V arbitrarily chosen) or on the pegboard, showing significantly less information in the vertical dimension on the pegboard (***$P < 0.0001$). (**e**) Diagram of the pegboard, showing the analysis layers (labeled according to a hypothetical cell with field peak in the central layer). (**f**) Percentages of firing fields spanning different vertical extents (specified as layer span).

(R = 0.39, not significant). However, subfield spacing and stripe spacing values, which were also similar (68 ± 4 cm and 66 ± 3 cm, respectively; t_{24} = 0.38, not significant), did correlate (R = 0.71, $P < 0.05$). One cell expressed three stripes for which the inter-stripe spacings were unequal, which is consistent with the stripes being randomly oriented cross-sections through a hexagonal columnar array of firing fields (see below).

Although the firing fields appeared as stripes, the vertical rate analysis found, as for place cells, a decline across layers, even when the peak was excluded (**Supplementary Fig. 3**; $R = -0.59$, $P < 0.0001$), indicating some rate modulation by height. This suggests that either the stripes are actually long thin ovals or there is some thinning of the fields, perhaps owing to edge effects, at the top and bottom borders of the apparatus.

The observations on the pegboard were made on a two-dimensional environment. In experiment 2, we made recordings on a helical track (**Fig. 3** and **Supplementary Fig. 1b**), which allows animals to move in three dimensions, albeit with yoking of horizontal and vertical displacements. Rats shuttled between the top and bottom of the transparent helix several times per session, circumnavigating five coils (in the case of four rats with hippocampal electrodes and six with entorhinal) or six coils (in the case of two rats with hippocampal electrodes). Horizontal position was recorded by an overhead camera that could see the rat's head-mounted LED through the clear plastic apparatus, and vertical position was derived by counting the number of coils circumnavigated. For position analyses, we compared the real place and grid cells against 'dummy' cells that were constructed by selecting a field for each coil at random from the complete data set, in order to abolish between-coil correlations. We compared data from the helix with data from the flat environments from experiment 1.

Place fields on the helix

For the purposes of description, a 'run' is an excursion from top to bottom and a coil is a circumnavigation, which could occur at any level. Separate analyses were run for each direction, but as the results were similar a combined analysis is reported throughout. Analyses for the five-coil and six-coil version of the helix are combined unless stated otherwise.

Seen from above, with all the coils collapsed together, place cells produced spatially localized fields (**Fig. 3a**, left). To determine the dimensional characteristics of the firing fields, each coil of the helix was unwound to produce a linear, 64-bin plot of position (**Supplementary Fig. 9**). Place cells usually fired differently on upward (counterclockwise) versus downward (clockwise) runs, with 92% being strongly modulated in rate, position or both (**Supplementary Results**). Therefore, we treated upward and downward runs as different data sets.

Place cell firing recurred on multiple coils (**Fig. 3a**; see **Supplementary Fig. 10** for the complete data set). The firing locations on the different coils were highly correlated (R = 0.500), which was in contrast with the control set of dummy place cells (R = 0.005; $Z_{N=191}$ = 9.9, $P < 0.0005$; Mann–Whitney test), and only small lateral shifts of the coils (4.6 bins) compared with the dummy cells (16.3 bins; $Z_{N=191}$ = 9.8, $P < 0.0005$; Mann–Whitney test) were required to maximize the between-coils correlation (**Fig. 3c**). Firing thus recurred at the same relative location and did not 'remap' between coils. Henceforth, we treated fields as unitary, vertical ellipses, with height being the major axis and extent along the track being the minor axis.

The axis dimensions, and aspect ratios, of the firing fields are shown in **Figure 3d** and summarized in **Table 1**. The minor axis averaged 40 ± 2 cm, larger than the minor axis on the flat (21 ± 1 cm; t_{154} = 5.64, $P < 0.0001$) but similar to the 38 ± 2 cm major axis of place fields on the flat arenas (t_{154} = 0.5, not significant). Vertical field extent averaged

© 2011 Nature America, Inc. All rights reserved.

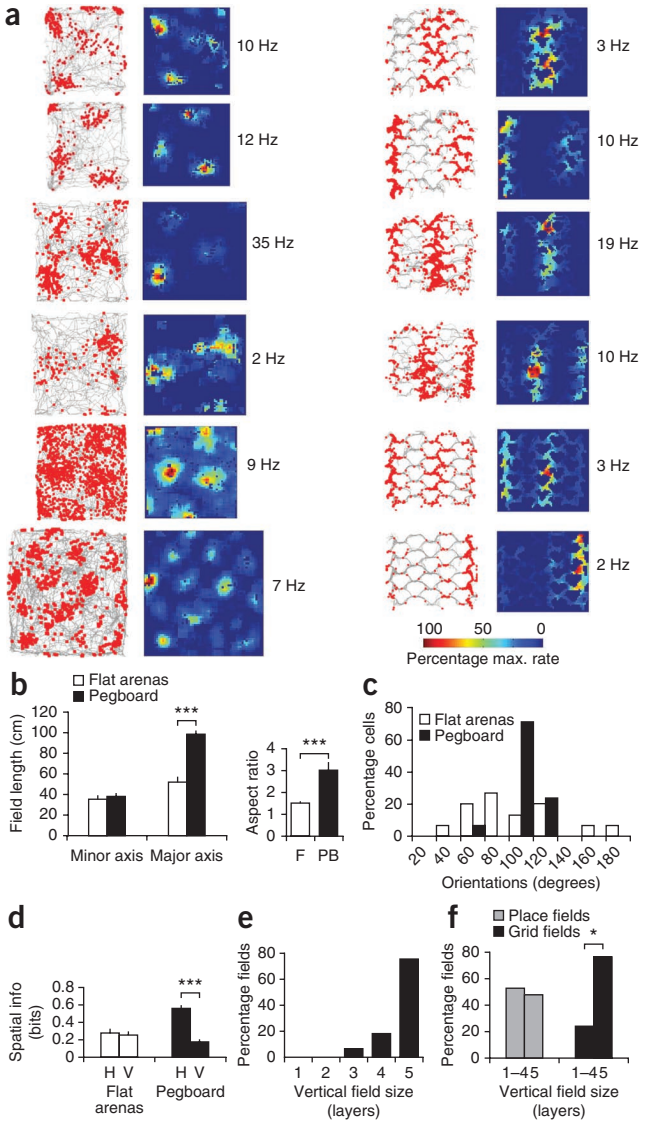

Figure 2 Grid fields on the pegboard. (**a**) Firing fields of 12 grid cells on the flat arenas (left plots) and on the vertical pegboard (right plots). Fields are as described in **Figure 1a** except that spikes are red. In the flat environments, firing fields were multiple and arranged approximately in a hexagonal close-packed array. On the pegboard, by contrast, the fields tended to be aligned in one or more vertical stripes. Peak rates (Hz) are shown beside the plots. The color bar shows percentages of peak firing. (**b**) Field sizes and aspect ratios (mean ± s.e.m.). On the pegboard, and in contrast with the place cells (**Fig. 1b**), the major axis increased in size whereas the minor axis did not, with a consequent increase in aspect ratio (***$P < 0.0001$). (**c**) Orientation of the grid fields, illustrated as in **Figure 1c**. (**d**) Spatial information content (mean ± s.e.m.) as shown in **Figure 1d** (***$P < 0.0001$). (**e**) Percentages of firing fields having different vertical extents (specified as layer span). (**f**) Comparison of number of place and grid fields spanning all five layers versus place and grid fields spanning fewer than five (*$P < 0.05$).

69 ± 2 cm, which was significantly greater than the horizontal dimension (40 ± 2 cm; $t_{204} = 11.8$, $P < 0.0001$). It was, however, less than the major axis of place fields on the pegboard (78 ± 3 cm; $t_{141} = 2.6$, $P < 0.01$), perhaps because the helix was shorter. The aspect ratio for place fields on the helix was 2.1 ± 0.1, which was similar to that of the flat arenas (2.0 ± 0.1; $t_{154} = 1.00$, not significant) but less than that of the pegboard (2.4 ± 0.2; $t_{141} = 1.39$, $P < 0.05$). Fields on the five-coil helix tended to be smaller than on the six-coil helix in both horizontal extent (35 ± 3 cm and 45 ± 4 cm, respectively; $t_{101} = 2.2$, $P < 0.05$) and vertical extent (63 ± 2 cm and 75 ± 2 cm, respectively; $t_{101} = 4.3$, $P < 0.0001$) and thus did not differ in their aspect ratios (2.2 ± 0.1 and 2.1 ± 0.1, respectively; $t_{101} = 0.4$, not significant).

The vertical distribution of place field peaks is shown in **Figure 3e** and **Supplementary Figure 11**. Although there were slightly more at the top and bottom, this distribution did not differ from uniform ($\chi^2_{2,N=215} = 5.1$, not significant). Cells with differing vertical spreads were counted as for the pegboard, using coils instead of layers. Whereas 32 fields spanned all five coils, only 18 spanned fewer than five (**Fig. 3f**). Thus, as on the pegboard, fields on the helix tended to occupy a long vertical extent, but did not always. Despite the elongation of the fields, place cell firing rates as a function of distance from the peak steadily attenuated (**Supplementary Fig. 3**; $R = -0.36$, $t_{462} = 8.25$, $P < 0.0001$), unlike dummy place cell firing rates ($R = -0.032$, $t_{406} = 0.64$, $P > 0.05$). In summary, place cells seemed to be partially modulated by vertical travel distance on the helix, as they were on the pegboard.

Grid fields on the helix

Grid cell firing patterns, when viewed from above, resembled those seen in the open-field arenas: that is, they typically had more than one

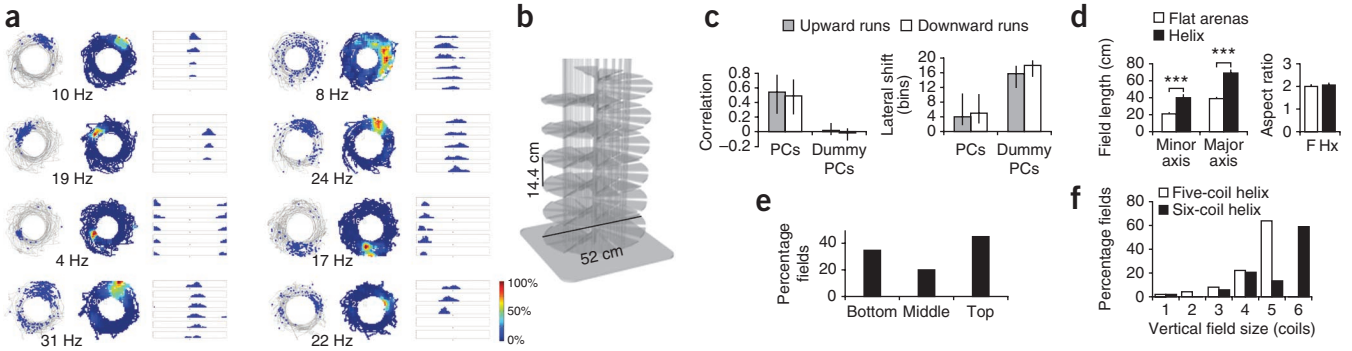

Figure 3 Place fields on the helix. (**a**) Firing patterns of eight place cells on the track, as seen from overhead (left and middle; details as in **Fig. 1a**) or decomposed into firing rate histograms from individual coils (right). Data represent upward or downward runs, but not both. Peak rates (Hz) are shown in black text for the overhead rate maps. The color bar shows percentages of peak firing. (**b**) Schematic of the helical track. (**c**) Between-coil field correlation (median ± quartiles) for place cells (PCs) versus dummy place cells (left) and lateral shift (median ± quartiles) that maximized between-coil correlations for place fields and dummy place fields (right). (**d**) Major (long or vertical) and minor (short or horizontal) field axes (left), and aspect ratios (right), for place fields on the helix versus the flat environments (mean ± s.e.m.; ***$P < 0.0001$; F, flat; Hx, helix). (**e**) Distribution of place field peaks across the vertical extent of the helix. (**f**) Comparison of place field size for the five-coil and six-coil configurations of the track.

© 2011 Nature America, Inc. All rights reserved.

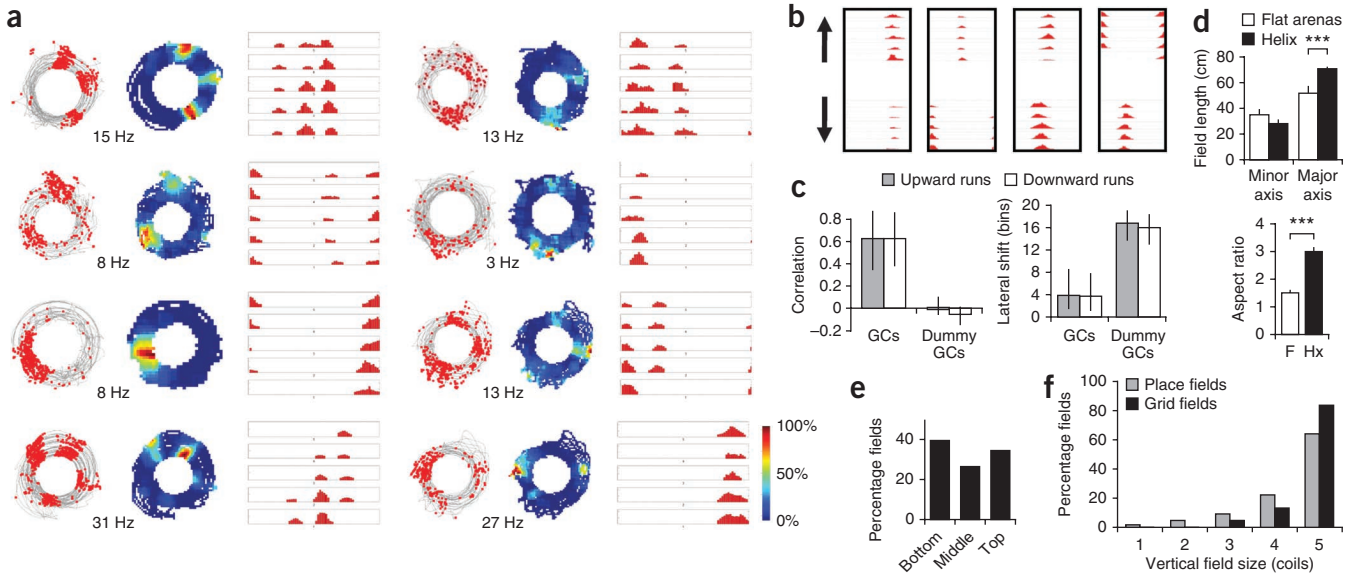

Figure 4 Grid fields on the helix. (**a**) Firing patterns of eight grid cells on the helix (details as in **Fig. 3a** but with spikes in red). Peak rates (Hz) are shown in black text for the overhead rate maps. The color bar shows percentages of peak firing. (**b**) Grid cell coil-by-coil rate histograms, showing upward and downward runs separately for four cells that showed significant directional modulation. (**c**) Between-coil field correlation (median ± quartiles) for grid cells (GCs) versus dummy grid cells (left), and lateral shift (median ± quartiles) that maximized between-coil correlations for grid fields and dummy grid fields (right), decomposed into upward and downward runs. (**d**) Major (long or vertical) and minor (short or horizontal) field axes (left) and aspect ratios (right) for grid fields on the helix versus the flat environments (mean ± s.e.m.; ***$P < 0.0001$; F, flat; Hx, helix). (**e**) Distribution of grid field peaks across the vertical extent of the helix. (**f**) Vertical field size comparison for place versus grid cells, showing increased tendency for grid cells to have fields that span the entire vertical extent of the helix.

activity peak (**Fig. 4a**; see **Supplementary Fig. 12** for the complete data set). Like place cells, grid cells were frequently modulated by direction of run (**Fig. 4b** and **Supplementary Results**), and so we again analyzed upward and downward runs separately and compared real data with dummy data.

Position analysis confirmed that firing recurred at the same place on each coil (correlations $R = 0.63$ and $R = -0.01$ for grid cells and dummy grid cells, respectively, $Z_{N=105} = 8.6$, $P < 0.0005$; lateral shifts = 3.9 and 16.7 bins for grid cells and dummy cells, respectively, $Z_{N=105} = 8.1$, $P < 0.0005$; both Mann–Whitney test; **Fig. 4c**). The horizontal extent of grid fields along the track (minor axis) averaged 28 ± 2 cm, which was not different from the minor axis on the flat (35 ± 4 cm; $t_{74} = 1.6$, not significant; **Fig. 4d** and **Table 1**). The inter-peak distance between fields on the track ranged from 19 to 66 cm (mean ± s.e.m. = 44 ± 2 cm). Vertical field extent averaged 69 ± 1 cm, which was greater than the horizontal dimension ($t_{104} = 17.6$, $P < 0.0001$) and greater than the major axis of fields on the flat ($t_{74} = 5.1$, $P < 0.0001$). Like the place fields, this was, however, less than the vertical extent of grid fields on the pegboard (98 ± 4 cm; $t_{68} = 7.82$, $P < 0.0005$). The aspect ratio was 2.9 ± 0.1 overall, which—in contrast with the place fields—was significantly different from the aspect ratio on the flat arenas (1.5 ± 0.1; $t_{74} = 6.33$, $P < 0.0001$) and indistinguishable from the aspect ratio on the pegboard (3.0 ± 0.4; $t_{68} = 0.0$, not significant). An ANOVA comparing aspect ratios on the flat arenas versus the helix for 23 grid fields and 23 randomly chosen place fields (92 fields altogether) found a main effect of cell type ($F_{1,88} = 6.6$, $P < 0.05$), a main effect of environment ($F_{1,88} = 23.6$, $P < 0.001$) and a significant interaction ($F_{1,88} = 26.1$, $P < 0.001$). *Post hoc* pairwise comparisons (Tukey's test) found that place field aspect ratios did not differ between flat arenas and helix (ratios both 1.9), but grid fields differed significantly (ratios of 1.5 ± 0.3 on the flat and 2.9 ± 1.0 on the helix; $t_{44} = 6.66$, $P < 0.0001$). Furthermore, on the helix, grid field aspect ratios were significantly greater than those of place fields ($t_{44} = 4.27$, $P < 0.0001$). Therefore, grid fields were more elongated than place fields on the helix.

The vertical distribution of grid field peaks is shown in **Figure 4e** and **Supplementary Figure 11**. As with place fields, there were slightly more at the top and bottom, but not significantly more ($\chi^2_{2,N=121} = 0.82$). We counted the numbers of fields with different coil spans, as for place cells. In contrast with the place cells, grid cells were more inclined to fire on all coils, and firing very rarely if ever fell to zero on any coil (**Fig. 4f** and **Supplementary Fig. 12**). Thus, of the 53 primary grid fields, 44 fired on all five coils, whereas only 7 fired on four coils and 2 on three coils. A chi-squared analysis comparing fields spanning five versus fewer than five coils between place and primary grid fields found a significant difference ($\chi^2_{1,N=103} = 4.81$, $P < 0.05$). Thus, place cells showed some modulation by height, but grid cells showed less modulation. Nevertheless, grid cell firing rates did also fall away progressively from the peak (**Supplementary Fig. 3**; $R = -0.30$, $t_{314} = 5.54$, $P < 0.0001$), unlike dummy grid firing rates ($R = 0.022$, $t_{206} = 0.32$, $P > 0.05$).

Histological analysis showed that of the ten posteriorly implanted animals, seven had clearly identifiable electrode tracks. Of these, six were in either medial entorhinal cortex or parasubiculum (**Supplementary Fig. 13**) and one was in the subiculum or dentate molecular layer.

DISCUSSION

Our study shows that place and grid cells showed less sensitivity to height than to horizontal displacement, and it thus seems that 'neural odometry' was selectively impaired in the vertical dimension. Most notably, grid cells, which show periodic firing in the horizontal plane, showed no vertical periodicity. The fact that environments of differing structure elicited different locomotor behavior but produced similar results suggests that the neural representation of allocentric space has intrinsically different properties in the vertical dimension from those in the horizontal, and is therefore anisotropic.

© 2011 Nature America, Inc. All rights reserved.

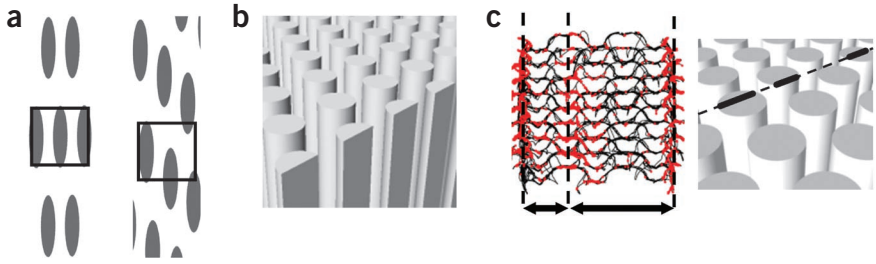

Figure 5 Hypotheses concerning the firing patterns observed in the present experiment. (**a**,**b**) Two hypotheses about why grid fields appear vertically elongated on the pegboard. (**a**) The stripes could result from vertical stretching of an intrinsically hexagonal field array (shown for arrays at two different orientations), which is then sampled by the pegboard (squares). (**b**) The stripes could result from transection of an intrinsically columnar field array. (**c**) Observation of a cell with variable inter-stripe spacing favors the columnar-transection hypothesis (see main text for details).

Although both place and grid fields were vertically elongated, they were nevertheless partially height-modulated on both apparatuses, with place cells being more modulated than grid cells. This modulation suggests that height is encoded by these cells, but in a different way. The difference may be merely one of scale: had we used very tall environments, we might have seen grids occurring over a very large scale, producing apparent stripes on a small apparatus but revealing periodicity on a large one (**Fig. 5a**). However, it may be that the difference is qualitative rather than quantitative: that is, the way in which firing is modulated differs in vertical versus horizontal dimensions. Place fields have been shown to respond to qualitative as well as quantitative variations in environmental stimuli, as evidenced by their altered firing in response to changes in 'context' (reviewed in ref. 10). Given that changes in an animal's height above ground produce changes in qualitative contextual aspects of the environment over and above mere metric changes, it may be that these are what modulate firing in the vertical dimension. Such contextual modulation could explain why there is a dissociation between the sensitivity of grid cells and place cells to height: possibly, place cells are informed about height, through their contextual inputs, in a way that grid cells are not.

There have been earlier suggestions that encoding of the vertical dimensions may be non-metric in place cells. Initial studies of place cells on a sloping or vertically translated surface found evidence of sensitivity to vertical displacement[11–13] and also to tilt[13] but little evidence of true metric encoding. However, this could have been due to the strong salience of local cues conferred by the environment surfaces, causing odometry to be dominated by the floor. By contrast, on our pegboard apparatus, the wall provided the dominant (and indeed only) surface: odometry was preserved in the horizontal dimension, despite the absence of a horizontal surface, but was impaired in the vertical dimension, despite the presence of a vertical surface. Thus, the impaired vertical odometry does not seem to be due to the surface structure of the environment.

The pattern of grid cell stripes on the pegboard is consistent with the stripes being cross sections through a hexagonal close-packed columnar array (**Fig. 5b**), which could explain the irregular inter-stripe spacing (**Fig. 5c**). However, the stripes are also reminiscent of previous findings[14] of directionally dependent stripe-like activity on a hairpin maze composed of repeating segments. In that experiment, instead of a continuous pattern of grid fields, the grid cell responses in the maze repeated on each successive entry into identical maze sub-compartments, introducing a discontinuity in the grid pattern that apparently indicated failure of the cells to take into account (that is, to path integrate) distance traveled in the direction orthogonal to the linear compartments. Notably, cells were highly directional in this apparatus, suggesting that the two opposing directions of travel were treated as different environments, or 'contexts'. However, fields on the pegboard were not directional, nor did rats execute such stereotyped movements that their trajectories could be broken up into compartment-like blocks. Furthermore, on the helix, unlike the discontinuous grid pattern in the hairpin maze, we observed a continuous, repeating pattern of grid bumps. The differences occurring between our experiments and the hairpin maze work[14] suggest that the phenomena may be different. However, the common feature of pattern repetition seen in these environments may reflect the common feature of impaired path integration in a direction orthogonal to the main direction of travel.

The results on the helix similarly resemble previously published findings[15] that place-field patterns repeat on successive laps of a horizontal spiral. The cells failed to encode the lateral translation that occurred with each successive lap of the spiral, in a manner analogous to how our cells failed to encode the vertical translation that occurred on each lap. This suggests a general hypothesis: that path integration does not function effectively for movement in a dimension that is perpendicular to the long axis of the animal (such as, for surface-dwelling animals, the vertical dimension). An analogous finding has been reported in head direction cells, which encode directions only in the plane of locomotion[16]; this apparently produces a planar compass signal, but one that can be oriented vertically if the animal—unlike on our pegboard—orients its body plane vertically.

Impaired vertical odometry might result from the lesser amount of visual information about vertical travel. We think it unlikely that vertical cues are more impoverished, as the experimental rooms possessed many features at multiple vertical levels (shelves, doors, and so on; **Supplementary Fig. 1**), and in any case, on the horizontal plane, place and grid fields are usually well formed even when the only source of visual discontinuity is a single landmark. We therefore suggest that impaired vertical path integration is the likelier explanation. Models of grid cell generation postulate a metric process by which interfield spacing is computed[17–19]: in a similar way to the metric models of place field generation, these models could account for the vertical elongation by presuming a deficient or absent distance-calculating process for travel in the direction perpendicular to the plane of the animal's head and body.

The generality of the present findings is a question for future research. In both apparatuses, rats were constrained in their movements, and it may be that this impaired the ability of the allocentric spatial system to form a volumetric representation. Alternatively, because rats are surface-traveling animals, it may be that during the course of evolution the system has, in rats and other surface-traveling species, lost some of its ability to represent space volumetrically (that is, with metric information in all three dimensions), even in a volumetric environment. However, it is also possible that the planar character of the cognitive map is a general feature of animals in all settings. Representing three dimensions volumetrically is computationally highly complex, partly because it requires many more representational units (scaling as the square of the equivalent horizontal component) and also—more importantly—because it requires an integrated three-dimensional compass with four degrees of freedom (three for heading—one in each rotational plane—plus one for orientation of the head and body around the long axis), for which there is no evidence in any animal at present. As humans, our subjective sense of three-dimensional space feels as though it is fully integrated in all three

© 2011 Nature America, Inc. All rights reserved.

dimensions. However, experiments in zero gravity have found that when subjects can move freely in all directions, they nevertheless tend to impose a reference 'horizontal' on the environment[20]. This suggests that our own internal representation of space may also be planar and that our sense of having a complete three-dimensional spatial map may be an illusion. This has important consequences for understanding human exploration and mapping of three-dimensional spaces such as undersea, air, space and—more recently—virtual reality.

METHODS

Methods and any associated references are available in the online version of the paper at http://www.nature.com/natureneuroscience/.

Note: Supplementary information is available on the Nature Neuroscience website.

ACKNOWLEDGMENTS

The work was supported by grants from the Wellcome Trust to K.J.J., the European Commission Framework 7 ('Spacebrain') to K.J.J. and Axona Ltd, and a National Science Foundation grant (no. IOS-0725001) to A.A.F. We thank E. Kelemen for help designing and M. Shkop for constructing the helical track, E. Leeper for building the pegboard arena, M. Witter for advice on histology and C. Barry and F. Cacucci for comments on the manuscript.

AUTHOR CONTRIBUTIONS

R.H., M.A.V. and A.J. contributed equally to the work. R.H. and M.A.V. implanted electrodes, recorded and analyzed the bulk of the data and wrote most of the Online Methods. A.J. recorded the bulk of the pegboard data and contributed analysis and the Online Methods. A.A.F. conceived the helical track, oversaw its construction and advised on data analysis and interpretation. K.J.J. conceived and gained funding for the overall research program, designed the pegboard and oversaw its construction, supervised the data collection and analysis and wrote the Introduction and Discussion.

COMPETING FINANCIAL INTERESTS

The authors declare competing financial interests: details accompany the full-text HTML version of the paper at http://www.nature.com/natureneuroscience/.

Published online at http://www.nature.com/natureneuroscience/.
Reprints and permissions information is available online at http://www.nature.com/reprints/index.html.

1. Burgess, N. Spatial cognition and the brain. *Ann. NY Acad. Sci.* **1124**, 77–97 (2008).
2. Moser, E.I., Kropff, E. & Moser, M.B. Place cells, grid cells, and the brain's spatial representation system. *Annu. Rev. Neurosci.* **31**, 69–89 (2008).
3. Hafting, T., Fyhn, M., Molden, S., Moser, M.B. & Moser, E.I. Microstructure of a spatial map in the entorhinal cortex. *Nature* **436**, 801–806 (2005).
4. Boccara, C.N. *et al.* Grid cells in pre- and parasubiculum. *Nat. Neurosci.* **13**, 987–994 (2010).
5. Barry, C., Hayman, R., Burgess, N. & Jeffery, K.J. Experience-dependent rescaling of entorhinal grids. *Nat. Neurosci.* **10**, 682–684 (2007).
6. O'Keefe, J. & Nadel, L. *The Hippocampus as a Cognitive Map* (Clarendon Press, 1978).
7. Jeffery, K. Navigating in a 3D world. in *Animal Thinking: Contemporary Issues in Comparative Cognition* (eds. Menzel, R. & Fischer, J.) (MIT Press, in the press).
8. Hartley, T., Burgess, N., Lever, C., Cacucci, F. & O'Keefe, J. Modeling place fields in terms of the cortical inputs to the hippocampus. *Hippocampus* **10**, 369–379 (2000).
9. Skaggs, W.E., McNaughton, B.L., Gothard, K.M. & Markus, E.J. An information-theoretic approach to deciphering the hippocampal code. *Adv. Neural Inf. Process. Syst.* **5**, 1031–1037 (1993).
10. Jeffery, K.J. Integration of the sensory inputs to place cells: what, where, why, and how? *Hippocampus* **17**, 775–785 (2007).
11. Knierim, J.J. & McNaughton, B.L. Hippocampal place-cell firing during movement in three-dimensional space. *J. Neurophysiol.* **85**, 105–116 (2001).
12. Knierim, J.J., McNaughton, B.L. & Poe, G.R. Three-dimensional spatial selectivity of hippocampal neurons during space flight. *Nat. Neurosci.* **3**, 209–210 (2000).
13. Jeffery, K.J., Anand, R.L. & Anderson, M.I. A role for terrain slope in orienting hippocampal place fields. *Exp. Brain Res.* **169**, 218–225 (2006).
14. Derdikman, D. *et al.* Fragmentation of grid cell maps in a multicompartment environment. *Nat. Neurosci.* **12**, 1325–1332 (2009).
15. Nitz, D.A. Path shape impacts the extent of CA1 pattern recurrence both within and across environments. *J. Neurophysiol.* **105**, 1815–1824 (2011).
16. Stackman, R.W., Tullman, M.L. & Taube, J.S. Maintenance of rat head direction cell firing during locomotion in the vertical plane. *J. Neurophysiol.* **83**, 393–405 (2000).
17. McNaughton, B.L., Battaglia, F.P., Jensen, O., Moser, E.I. & Moser, M.B. Path integration and the neural basis of the 'cognitive map'. *Nat. Rev. Neurosci.* **7**, 663–678 (2006).
18. O'Keefe, J. & Burgess, N. Dual phase and rate coding in hippocampal place cells: theoretical significance and relationship to entorhinal grid cells. *Hippocampus* **15**, 853–866 (2005).
19. Fuhs, M.C. & Touretzky, D.S. A spin glass model of path integration in rat medial entorhinal cortex. *J. Neurosci.* **26**, 4266–4276 (2006).
20. Tafforin, C. & Campan, R. Ethological experiments on human orientation behavior within a three-dimensional space—in microgravity. *Adv. Space Res.* **14**, 415–418 (1994).

© 2011 Nature America, Inc. All rights reserved.

ONLINE METHODS

Subjects and apparatus. We implanted rats with tetrodes aimed at the dorsal CA1 region of the hippocampus (n = 12), dorsomedial entorhinal cortex (n = 9) or postsubiculum (n = 1; this was from another experiment, but it yielded a grid cell that may have been in the subiculum or dentate molecular layer[21]). All procedures were performed under UK Home Office license authority according to the Animals (Scientific Procedures) Act 1986.

The pegboard (**Fig. 1e** and **Supplementary Fig. 1a**) comprised a vertically oriented wooden board 121 × 121 cm square, studded at 10–20 cm intervals with projecting wooden dowels (17 cm × 9 mm). The helical track (**Fig. 3b** and **Supplementary Fig. 1b**) comprised clear acrylic plastic triangular steps anchored at the innermost end and winding in a right-handed spiral around a central core, making five or six complete turns, each of pitch 14.4 cm. The helix was 52 cm in diameter and the central core was 33 cm in diameter. A horizontally aligned camera viewed the pegboard, and a downward-pointing ceiling-mounted camera viewed the helix. Control environments were square or circular arenas 60–200 cm across.

Electrode implantation and recording. Recording electrodes were four tetrodes mounted in a microdrive (Axona) and aimed at the hippocampus (coordinates −3.8–4.0 mm antero-posterior, 2.2–2.5 mm medio-lateral and 1.5 mm dorso-ventral), dorsomedial entorhinal cortex (tetrodes angled 6–10° in the parasagittal plane and implanted at 0.1–0.3 mm anterior to the transverse sinus, 4.0–4.5 mm medio-lateral and 1.5–2.0 mm dorso-ventral) or postsubiculum (−6.7 mm antero-posterior, 2.8 mm medio-lateral and 1.6 mm dorso-ventral).

After recovery, recordings were made using an Axona 16-channel DacqUSB system. After place or grid cells were isolated, we placed the rats on one of the environments to explore for food while spike data were collected. On the pegboard, rats foraged by clambering over the pegs (**Fig. 1** and **Supplementary Fig. 1**) for 10–30 min. On the helical track, rats repeatedly ran from the bottom to the top and back again, being rewarded at both ends. Trials consisted of 20 min or 14 runs, whichever was shorter.

Data analysis. We isolated units using a cluster cutting program (Tint, Axona). Hippocampal cells were considered to be place units if their activity had a peak rate >1 Hz, produced >50 spikes and showed, on the open field or pegboard, spatially localized firing (coherence value >0.66) or showed, on the helical track, firing on more than one run. Cortical cells were considered to be grid cells if their activity had a peak rate >1 Hz and had localized firing in at least one location that remained stable in at least one environment.

We constructed position-normalized firing rate maps, defining the field containing the peak firing as the 'main field'. For open field and pegboard analyses, we used smoothed rate maps to derive field length and width, aspect ratio, orientation and—for grid cells—inter-peak spacing (when analyzing multiple fields) and symmetry order.

Rate maps. For each cell, firing rate maps were constructed by dividing the entire camera viewing area into 64 × 64 bins, each approximately 2 × 2 cm, and then dividing the total number of spikes in each bin by the dwell time. The resulting maps were smoothed with a boxcar algorithm (width, 5 bins on the helix or 7 bins on the open field and pegboard). The fields were then extracted by a thresholding process in which patches of at least five consecutive bins with firing greater than 15% of the peak rate were considered to be part of the field and the rest were set to zero.

Spatial analysis. For the pegboard, we implemented an algorithm to coalesce fields that had been fragmented by the more interrupted trajectory of rats on that apparatus, and then applied the same algorithm to the open field data. The algorithm was as follows: within the main field, each bin in turn was tested to check whether, within a 5 × 5 bin range, any nearby bin contained above-threshold firing. If so, it was assumed this bin belonged to the main field, despite the slight discontiguity, and it was thus included in the main field. This procedure was repeated twice. This algorithm failed when applied to grid fields from cells with small grid spacing in an open-field environment. Thus, if more than one peak was selected as the main field, these data were not included in the data set for analysis of field size and orientation but were still analyzed for symmetry.

Visited bins within the main field were then used to calculate field properties. The major and minor axes (length and width, respectively) of the fields were extracted using Matlab (R2008B; The MathWorks) and then used to calculate aspect ratio (ratio of major to minor field axes) and major-axis orientation of the main fields.

For the grid cells, two-dimensional autocorrelation maps[3] were generated by taking the smoothed firing rate map and repeatedly correlating it with itself after it was shifted in successive one-bin increments in x and y directions. Formally, the spatial autocorrelogram was defined as

$$r(\tau_x,\tau_y) = \frac{\eta\sum\lambda(x,y)\lambda(x-\tau_x,y-\tau_y)-\sum\lambda(x,y)\sum\lambda(x-\tau_x,y-\tau_y)}{\sqrt{\eta\sum\lambda(x,y)^2-\left(\sum\lambda(x,y)\right)^2}\sqrt{\eta\sum\lambda(x-\tau_x,y-\tau_y)^2-\left(\sum\lambda(x-\tau_x,y-\tau_y)\right)^2}}$$

where $r(\tau_x, \tau_y)$ is the autocorrelation between bins with an offset of τ_x and τ_y, $\lambda(x,y)$ is the firing rate in the bin located at (x,y) and η is the number of bins over which the estimate was made. For periodic patterns, the autocorrelograms are also periodic.

The spatial autocorrelograms were used to calculate both field spacing and field width for open field trials. (Note that an additional field width was also used for one analysis; see below.) Field spacing was calculated as the mean distance from the central point in the spatial autocorrelogram to the six nearest peaks. Field width was calculated as the diameter of the largest circle that contained all pixels in the central region above a threshold of 0.15.

Vertical rate analysis. To determine whether the observed vertical stretching on the pegboard was rate modulated, the pegboard was divided into five horizontal layers of equal size. For the main field, the layer on which a given cell fired maximally was given a value of 0, whereas layers above and below it were successively numbered positively, from 1 to a possible 4. Firing rates on all layers were converted to percentages of the peak rate. To determine whether firing rates declined steadily with increasing distance from the peak (as would be expected if they were modulated by height) or fluctuated randomly, we statistically compared firing rates by conducting a regression analysis of firing rate against distance (in layers) from the peak. Because the peak is fixed by definition at 100%, we excluded it from the analysis.

Spatial information. Skaggs' spatial information is a measure of the degree to which the firing of an individual cell can be used to predict the location of the animal[4]. Mutual information between firing rate R and environment X is defined as follows:

$$I(R\,|\,X) \approx \sum_i p(\mathbf{x}_i) f(\mathbf{x}_i) \log_2\left(\frac{f(\mathbf{x}_i)}{F}\right)$$

where $p(\mathbf{x}_i)$ is the probability of being in pixel $\mathbf{x}_i$, $f(\mathbf{x}_i)$ is the firing rate of the cell in pixel $\mathbf{x}_i$ and F is the overall firing rate of the cell.

This measure was used in three ways. First, a spatial information score for the two-dimensional smoothed firing rate map for each cell was obtained. Second, the smoothed firing rate map was collapsed horizontally such that each bin of the resulting linearized rate map was a mean of the firing rate of the bins collapsed into that bin. A separate spatial information score was then obtained from this linearized rate map. Finally, the same process was used except that rate maps were collapsed vertically instead of horizontally.

Symmetry analysis. To determine the symmetries of grid cell firing for horizontal and vertical environments, two symmetry analyses of grid cell firing patterns were undertaken, one rotational and one translational. These comprised a double autocorrelation procedure in which each autocorrelation map was rotated or translated and then re-correlated with the original, as follows.

Rotational symmetry was determined by adapting a previous method[22], cropping the autocorrelation maps to remove the central peak and the area outside the outermost of the six central peaks, and then rotating the map and re-correlating it with the original, in 1° increments up to the full 360°. The Pearson product moment correlation at each step was plotted on a graph of correlation against angle and zero-lag-averaged (window size, 30 bins) to remove minor

© 2011 Nature America, Inc. All rights reserved.

doi:10.1038/nn.2892

irregularities (**Supplementary Fig. 5**). The smoothed plot was then differentiated to identify peaks and troughs. The vertical distance between each peak and its adjacent troughs was calculated, and the number of times in a given plot that this difference exceeded a given threshold was counted for all thresholds ranging from 0 to 0.3. This provided a variable plot of peak number against threshold, where the definition of 'peak' varied from small irregularities in the symmetry plot (when the threshold was close to zero and the peak number was therefore high) to large fluctuations (when the threshold was high and excluded all but the tallest peaks). The plots thus obtained were compared between flat arena and pegboard conditions (**Supplementary Fig. 5**).

Translational symmetry was determined by sliding each autocorrelation map in one-bin increments and re-correlating the translated map with the original at each step. The collected values for a given translation direction (horizontal and vertical for the pegboard, and the arbitrarily chosen 'horizontal' and 'vertical' for the horizontal maps) were then averaged to produce a mean ± s.e.m. for each translation direction. In practical terms, this amounted to taking the central vertical and central horizontal columns of the re-correlated autocorrelation maps and collapsing each to a single, averaged value. For grid cells recorded on the pegboard, the vertical autocorrelation should have a constantly high value because every step of the autocorrelation procedure maps a stripe onto itself. Conversely, the horizontal value should be much lower because the stripes periodically map onto the inter-stripe spaces. The values for grid cells recorded in horizontal environments should also be much lower.

Stripe width and stripe spacing. For grid cells, we obtained stripe width by collapsing the smoothed data from the pegboard into one level, or row, of firing rates. This 'flat rate' was then thresholded at 15% peak rate. Stripe width was calculated for the main subfield as the number of bins on which there was firing multiplied by the bin size. For comparison with the grids on the flat arenas, we isolated the best horizontal grid field and subjected it to the same flattening and thresholding process as the stripe.

We calculated stripe spacing for all grid cells expressing more than one stripe by producing a linear spatial autocorrelation on the smoothed (but not thresholded) flat rate, made in one-bin steps. The stripe spacing was the distance between the main correlation peak and the next positive peak. To compare with the fields on the flat arenas, this distance was compared with the distance as obtained from the autocorrelograms.

Helical track analysis. We decomposed the helical track data into individual coils, which were then linearized (**Supplementary Fig. 9**) and divided into 64 firing-rate bins. The resulting plots were boxcar-smoothed (width = 5). A firing field comprised regions of at least five contiguous bins with firing above 15% of the peak rate. We compared real data against a control 'dummy' data set constructed from actual fields randomly chosen, for each coil independently, from the complete set.

We next examined horizontal and vertical field properties. Horizontally, two measures examined whether fields recurred in the same horizontal coordinates on different coils. First, we computed pairwise, between-coil, bin-for-bin Pearson's *R* correlations. Second, for each pair of coils we calculated the relative offset (measured in bins, with wraparound at the coil ends) that would maximize this correlation. For fields recurring in the same place on the two coils, this offset should approach zero.

For horizontal field size, we collapsed the helix by averaging the rates for each bin across all coils, smoothing as above and counting bins with firing above 15% of the peak rate. For grid cells with multiple fields, we averaged the data. Grid field spacing was determined from a linear spatial autocorrelation.

Vertical field analysis determined the vertical location of field peaks (chi-squared test of actual distribution of field numbers against a hypothetical uniform distribution), vertical extent of fields (expressed as centimeters or number of coils) and aspect ratio (height versus width). To determine whether firing was smoothly height modulated or fluctuated randomly, we used a regression analysis to compare firing rate (percentage peak rate) against distance in coils from the peak (excluding the peak itself). The coil on which a given cell fired maximally was given a value of 0, and coils above and below it were numbered according to their distance from coil 0. For place cells, in which some rats were run over six coils instead of five, data from the five-coil and the six-coil version were combined. The resulting scale thus ranged from 1 to 5 for place cells (given the maximum of six coils on the helix) and 1 to 4 for grid cells. The peak firing rates were expressed as a percentage peak rate, and a regression analysis was performed in the same way as for the pegboard.

Directionality. We assessed directionality (up and counterclockwise versus down and clockwise) by calculating coil-by-coil and overall correlations between upward and downward runs and averaging them. Cells with correlations below 0.4 were considered to be directional.

Histology. We used cresyl violet stains of 40-μm-thick brain sections to determine the locations of electrode tracks. Sections were cut coronally for implants aimed at the hippocampus and postsubiculum and sagittally for all others.

21. Leutgeb, J.K., Leutgeb, S., Moser, M.B. & Moser, E.I. Pattern separation in the dentate gyrus and CA3 of the hippocampus. *Science* **315**, 961–966 (2007).
22. Sargolini, F. *et al.* Conjunctive representation of position, direction, and velocity in entorhinal cortex. *Science* **312**, 758–762 (2006).

© 2011 Nature America, Inc. All rights reserved.